# POLAROGRAPHIC PEAKS OF THE THIRD KIND. V

E. V. Stenina, N. V. Nikolaeva-Fedorovich,
and I. I. Buraya

UDC 541.138.3:543.253

Adsorption of certain organic substances at the surface of a mercury droplet produces tangential movements of that surface and results in polarographic peaks of the third kind over the entire range of adsorption potentials for organic additives [1, 2]. These tangential movements and the peaks on I vs $\varphi$ curves (I denoting the current and $\varphi$ denoting the potential) at adsorption–desorption potentials have been first discovered by K. Doss and D. Venkatesan in solutions of sodium dioctyl-sulfosuccinate [3]. The possibility of polarographic peaks occurring together with surfactant concentration gradients within the volume adjoining the droplet has been considered in [4, 5]. S. Sathyanarayana has demonstrated [6, 7] sharp peaks in the case of camphor solutions. His interpretation of these peaks was based on the theory of droplet movements in a concentration-gradient field of an organic substance, a theory which had been developed earlier in [4, 5], but he associated this gradient with the presence of an electric field gradient rather than with the adsorption process. Such a hypothesis was incorrect, apparently, because the current peaks during camphor adsorption occurred in electrolytes of a high concentration. The authors of [3, 6, 7] thought that the potentials corresponding to peaks of the third kind should be the same as the potentials corresponding to desorption peaks for an organic substance along the curve of differential capacitance versus electrode potential.

A comparison between measurement data pertaining to the differential capacitance and the current flowing into a droplet [2, 8, 9] has revealed that the peaks may occur at any potential within the adsorption range for an organic substance when the degree of surface coverage is low.

An attempt to explain the mechanism which produces these peaks has been made in [10] on the basis of the theory developed in [4, 5]. According to that theory, the velocity of a droplet surface is approximately

$$v \simeq \frac{a\dfrac{\partial\sigma}{\partial x}}{2\mu+3\mu'+\gamma_\varepsilon+\gamma_a}, \tag{1}$$

where $\partial\sigma/\partial x = (\partial\sigma/\partial c)\cdot(\partial c/\partial x)$ denotes the gradient of surface tension along the droplet surface, $a$ denotes a quantity with the dimension of length, c denotes the volume concentration of the substance to be adsorbed, $\mu$ and $\mu'$ denote the viscosities of the solution and of mercury, respectively, $\gamma_\varepsilon$ and $\gamma_a$ denote the coefficients of surface retardation by charges of the electric double layer and by the adsorbate layer, respectively.

The authors have suggested that surface concentrations are equalized by the mechanism of surface diffusion and that the inequality $\gamma_a \gg 2\mu + 3\mu' + \gamma_\varepsilon$ prevails, whereupon they have obtained the expression

$$v \simeq \frac{D_s}{2\Gamma}\frac{\partial c}{\partial x}\frac{\partial\Gamma}{\partial c}, \tag{2}$$

with $D_s$ denoting the surface diffusivity.

M. V. Lomonosov State University, Moscow. Translated from Élektrokhimiya, Vol. 11, No. 10, pp. 1613-1618, October, 1975. Original article submitted December 4, 1974.

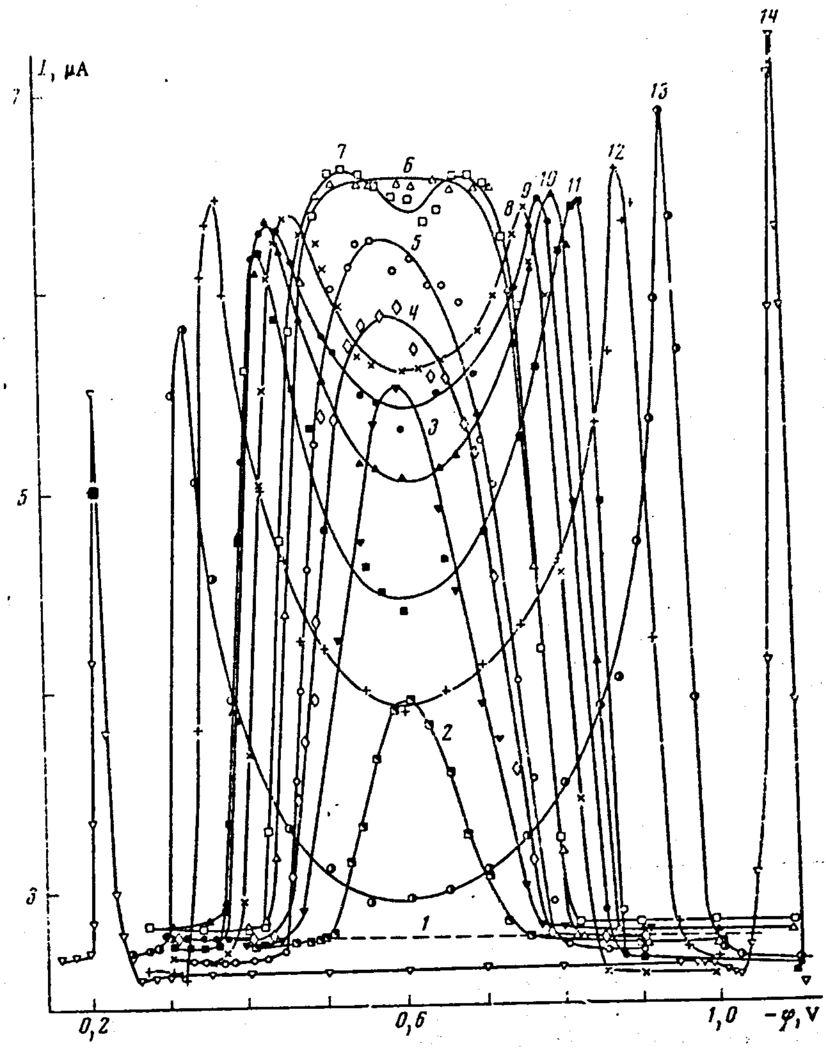

Fig. 1. Current I (μA) as a function of the potential $\varphi$ (V) during the reduction of $10^{-3}$ N $AgNO_3 + 1$ M $Na_2SO_4$ in the presence of 2-oxoadamantane in various concentrations (mole/liter): 1) 0; 2) $4.1 \cdot 10^{-5}$; 3) $4.25 \cdot 10^{-5}$; 4) $4.5 \cdot 10^{-5}$; 5) $5.5 \cdot 10^{-5}$; 6) $5.6 \cdot 10^{-5}$; 7) $5.75 \cdot 10^{-5}$; 8) $6 \cdot 10^{-5}$; 9) $7.0 \cdot 10^{-5}$; 10) $8.0 \cdot 10^{-5}$; 11) $9.0 \cdot 10^{-5}$; 12) $1.1 \cdot 10^{-4}$; 13) $1.5 \cdot 10^{-4}$; 14) $3.3 \cdot 10^{-4}$.

Calculations of $\partial\Gamma/\partial c$ as a function of $\varphi$ for adamantol and borneol in [10] have shown that the tangential velocity of a droplet surface depends on the electrode potential according to Eq. (2), which is analogous to the relation between the derivative $\partial\Gamma/\partial c$ and the potential.

It was of interest, therefore, to explore the appearance of polarographic peaks during the adsorption of organic substances with the simplest possible structure, without substitutions in the lateral chain. The authors selected for this 2-oxoadamantane with a diamond-like skeleton structure and its spatial isomers: twistane and 2-oxoisotwistane. The I vs $\varphi$ curves and the C vs $\varphi$ curves were measured by the method shown in [1, 11], with both the differential capacitance and the current into a droplet measured at the instant of droplet breakaway, both referred to the same lifetime of a droplet. All potentials in this study were measured in volts, relative to a standard calomel electrode.

The I vs $\varphi$ curves for a solution of $10^{-3}$ N $AgNO_3 + 1$ M $Na_2SO_4$ with various amounts of 2-oxoadamantane (OxAd) are shown in Fig. 1. With $4.1 \cdot 10^{-5}$ M OxAd added (Fig. 1, curve 2), near the zero-charge potential the current rises above its peak level without any OxAd added (Fig. 1, curve 1). As the OxAd concentration increases, this peak current rises further, and the potential range within which a polarographic peak of the third kind occurs becomes wider (Fig. 1, curves 3-6). Analogous results were obtained with solutions containing twistane and 2-oxoisotwistane. A further increase in the OxAd concentration produces a splitting of the peak and a decrease in the current within the range of the zero-charge potential (Fig. 1, curves 7-13).

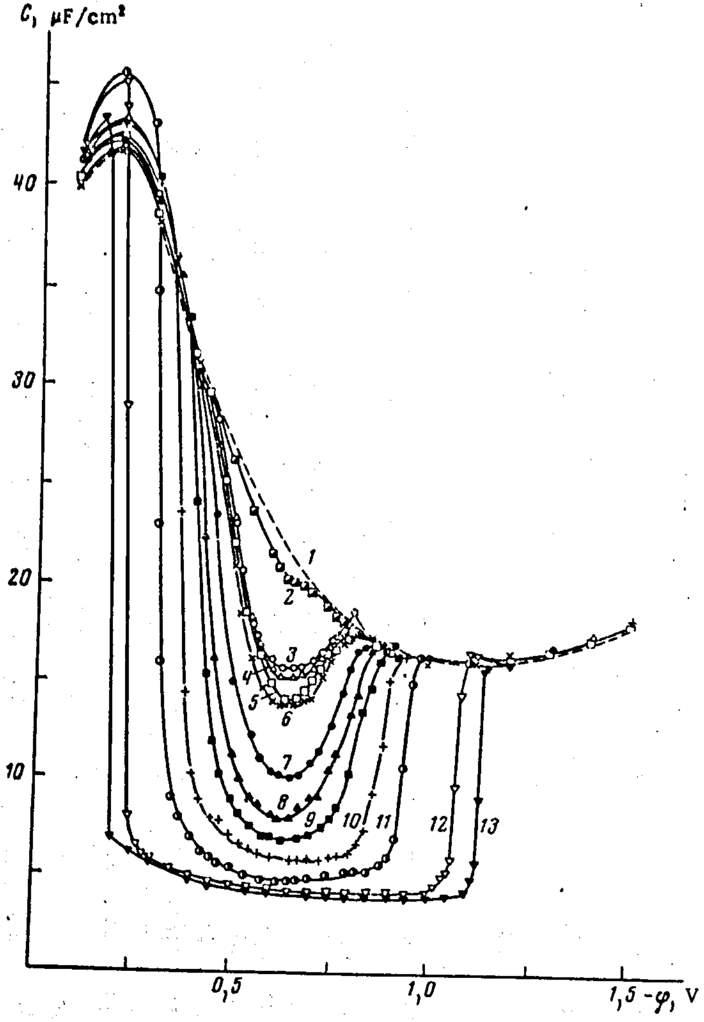

Fig. 2

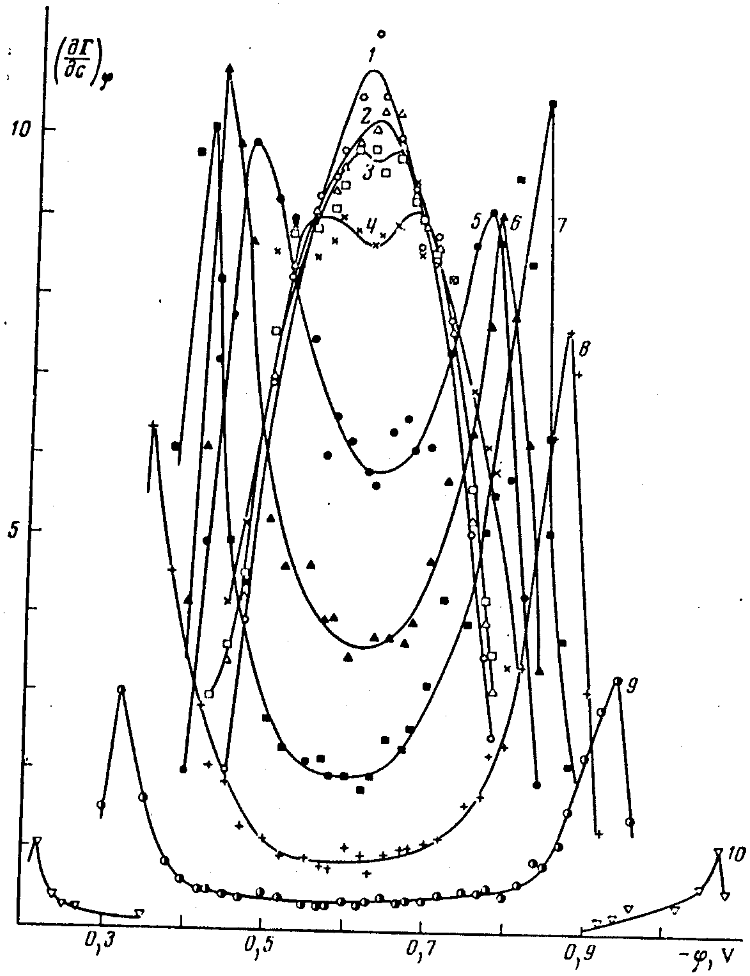

Fig. 3

Fig. 2. Differential capacitance C ($\mu$F/cm$^2$) as a function of the potential $\varphi$ (V), for 1 M $Na_2SO_4$ with 2-oxoadamantane added in various concentrations (mole/liter): 1) 0; 2) $4.5 \cdot 10^{-5}$; 3) $5.5 \cdot 10^{-5}$; 4) $5.6 \cdot 10^{-5}$; 5) $5.75 \cdot 10^{-5}$; 6) $6.0 \cdot 10^{-5}$; 7) $7.0 \cdot 10^{-5}$; 8) $8.0 \cdot 10^{-5}$; 9) $9.0 \cdot 10^{-5}$; 10) $1.1 \cdot 10^{-4}$; 11) $1.5 \cdot 10^{-4}$; 12) $3.3 \cdot 10^{-4}$; 13) $5.0 \cdot 10^{-4}$.

Fig. 3. Derivative $(\partial\Gamma/\partial c)_\varphi$ as a function of the potential $\varphi$ (V) for 1 M $Na_2SO_4$ with 2-oxoadamantane added in various concentrations (mole/liter): 1) $5.5 \cdot 10^{-5}$; 2) $5.6 \cdot 10^{-5}$; 3) $5.75 \cdot 10^{-5}$; 4) $6.0 \cdot 10^{-5}$; 5) $7.0 \cdot 10^{-5}$; 6) $8.0 \cdot 10^{-5}$; 7) $9.0 \cdot 10^{-5}$; 8) $1.1 \cdot 10^{-4}$; 9) $1.5 \cdot 10^{-4}$; 10) $3.3 \cdot 10^{-4}$.

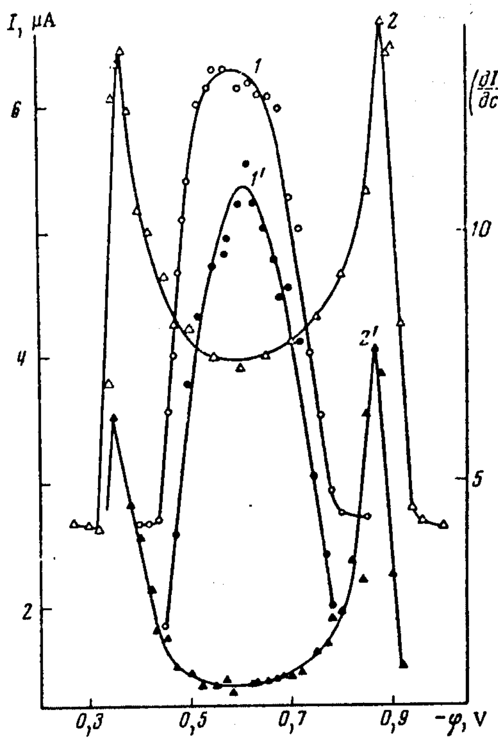

Fig. 4. Comparison between I vs $\varphi$ curves (1, 2) and $(\partial\Gamma/\partial c)_\varphi$ curves (1', 2'), for 2-oxoadamantane concentrations: 1,1') $5.5 \cdot 10^{-5}$ mole/liter, 2,2') $1.1 \cdot 10^{-4}$ mole/liter. Current I (μA), potential $\varphi$ (V).

The I vs $\varphi$ curves reveal two current peaks, at positive and at negative charges on the mercury surface, which shift in the direction of higher surface charges when the OxAd concentration increases and which, when the OxAd concentration is highest, appear only at the desorption potentials (Fig. 1, curve 14).

In order to calculate the values of $\partial\Gamma/\partial c$, we measured the C vs $\varphi$ curves (Fig. 2), the differential capacitance of the electric double layer at a dropping mercury electrode in 1 M $Na_2SO_4$ versus the electrode potential, with the same OxAd concentrations which had been used for plotting the I vs $\varphi$ curves. The trend of these C vs $\varphi$ curves for OxAd solutions is analogous to that of the C vs $\varphi$ curves which have been obtained earlier for solutions of camphor [6, 7], borneol [8, 9], and adamantanol [2]: No capacitance peaks appear on the C vs $\varphi$ curves, which is typical for adsorption processes along a Frumkin isotherm with the attraction constant $a \gg 2$. At sufficiently high OxAd concentrations, when the C vs $\varphi$ curves measured on a dropping mercury electrode appear balanced, the minimum value of the capacitance remains constant, while a further increase in the OxAd concentration only widens the range of adsorption potentials (Fig. 2, curves 12, 13). A comparison between the I vs $\varphi$ curves and the C vs $\varphi$ curves corresponding to low OxAd concentrations reveals that the range of potentials within which peaks of the third kind occur is the range of adsorption potentials for OxAd, with the maximum current peak corresponding to a degree of surface coverage $\theta \approx 0.3$–$0.5$. Then, probably, the areas with the surface tension reduced by the OxAd adsorption and the areas free of adsorbed molecules are in the most favorable ratio (Fig. 1). An increase in the OxAd concentration causes an increase in the degree of surface coverage within the adsorption region (Fig. 1, curves 7-13) and completely removes the peaks of the third kind from this range of potentials (Fig. 1, curve 14). Polarographic peaks of the third kind appear only, because at these potentials the degree of surface coverage may be anywhere from zero to unity.

For calculating $\partial\Gamma/\partial c = (\Gamma_m/c)(\partial\theta/\partial \ln c)_\varphi$ we used the value $\Gamma_m = 4.1 \cdot 10^{-10}$ mole/cm², which had been determined in [12] for adamantanol with a structure similar to that of OxAd. The derivative $(\partial\theta/\partial \ln c)_\varphi$ was determined graphically by differentiating the adsorption isotherms which had been calculated from C vs $\varphi$ curves (Fig. 2), according to the method in [10, 13-15].

The derivative $\partial\Gamma/\partial c$ as a function of the potential $\varphi$ for 1 M $Na_2SO_4$ with additions of OxAd is shown in Fig. 3. A comparison between Fig. 1 and Fig. 3 indicates that the $\partial\Gamma/\partial c$ vs $\varphi$ curves follow the same trend as the I vs $\varphi$ curves and that $\partial\Gamma/\partial c$ becomes maximum at the same potentials at which the current peaks occur at corresponding OxAd concentrations. Both sets of curves for solutions with certain OxAd concentrations are compared more precisely in Fig. 4. It seems that for solutions with the same OxAd content there definitely is a correspondence between the appearance of peaks of the third kind and the potential at which the slope of the Γ vs c curves becomes maximum, just as has been noted earlier in the case of borneol and adamantanol [10].

## LITERATURE CITED

1. A. N. Frumkin, E. V. Stenina, and N. V. Fedorovich, Élektrokhimiya, 6, 157 (1970).
2. A. N. Frumkin, E. V. Stenina, N. V. Fedorovich, G. N. Petukhova, V. A. Yusupova, and É. A. Shokova, Dokl. Akad. Nauk SSSR, 201, 1406 (1971).
3. K. Doss and D. Venkatesan, Proc. Indian Acad. Sci., 49, 129 (1959).
4. A. N. Frumkin, S. Sathyanarayana, and N. V. Nikolaeva-Fedorovich, Izv. Akad. Nauk SSSR, Otd. Khim. Nauk, 1977 (1962).

5. V. G. Levich and A. M. Kuznetsov, Dokl. Akad. Nauk SSSR, 146, 145 (1962).
6. S. Sathyanarayana, J. Electroanalyt. Chem., 10, 56 (1965).
7. S. Sathyanarayana and K. Baikerikar, J. Electroanalyt. Chem., 21, 449 (1969).
8. A. N. Frumkin, E. V. Stenina, N. V. Nikolaeva-Fedorovich, G. N. Petukhova, and V. A. Yusupova, Rev. Roumaine Chim., 17, 155 (1972).
9. E. V. Stenina, N. V. Nikolaeva-Fedorovich, G. N. Petukhova, and V. A. Yusupova, Vestn. Moskovsk. Univ., Ser. Khim., No. 1, 60 (1974).
10. A. N. Frumkin, N. V. Fedorovich, B. B. Damaskin, E. V. Stenina, and V. Krylov, J. Electroanalyt. Chem., 50, 103 (1974).
11. E. V. Stenina and N. V. Nikolaeva-Fedorovich, Élektrokhimiya, 6, 1723 (1970).
12. S. L. Dyatkina, B. B. Damaskin, E. V. Stenina, and N. V. Fedorovich, Élektrokhimiya, 10, 318 (1974).
13. G. A. Tedoradze and Ya. M. Zolotovitskii, Élektrokhimiya, 1, 201 (1965).
14. B. B. Damaskin, Élektrokhimiya, 1, 255 (1965).
15. B. B. Damaskin and S. L. Dyatkina, Élektrokhimiya, 7, 260 (1971).